Genetic analysis of a child with *SATB2*-associated syndrome and literature study

QIAN LIU, NAN-NAN FENG and LIN-JIAO CHEN

Center for Reproductive Medicine, Center for Prenatal Genetics, First Hospital of Jilin University, Changchun, Jilin 130021, P.R. China

Received July 2, 2022; Accepted February 23, 2023

DOI: 10.3892/etm.2023.12071

Abstract. The present study aimed to investigate clinical phenotype and genotype characteristics of a male child with *SATB2*-associated syndrome (SAS) and analyzed the relationship between these characteristics and the possible underlying genetic mechanism. His clinical phenotype was analyzed. Using a high-throughput sequencing platform, his DNA samples were subjected to medical exome sequencing, screened for suspected variant loci and analyzed for chromosomal copy number variations. The suspected pathogenic loci were verified by Sanger sequencing. He presented with phenotypic anomalies of delayed growth, delayed speech and mental development, facial dysmorphism showing the typical manifestation of SAS and motor retardation symptoms. Gene sequencing result analyses revealed a *de novo* heterozygous repeat insertion shift mutation in the *SATB2* gene (NM_015265.3) c.771dupT (p.Met258Tyrfs*46), resulting in a frameshift mutation from methionine to tyrosine at the amino acid site 258 and a truncated protein with 46 amino acids missing. The parents showed no mutation at this locus. This mutation was identified as the nosogenesis of this syndrome in children. To the best of the authors' knowledge, this is the first report on this mutation. The clinical manifestations and gene variation characteristics of 39 previously reported SAS cases were analyzed together with this case. The findings of the present study suggested severely impaired language development, facial dysmorphism and varying degrees of delayed intellectual development as the characteristic clinical manifestations of SAS.

Correspondence to: Dr Lin-Jiao Chen, Center for Reproductive Medicine, Center for Prenatal Genetics, First Hospital of Jilin University, 71 Xinmin Street, Changchun, Jilin 130021, P.R. China
E-mail: chenlinjiao@jlu.edu.cn

Key words: *SATB2* gene, glass syndrome, *SATB2*-associated syndrome, *de novo* mutation, hereditary disease

Introduction

SATB2-associated syndrome (special AT-rich binding protein 2-associated syndrome, SAS), also known as Glass syndrome (Glass syndrome; MIM # 612313), is an autosomal dominant disorder caused by mutations in the *SATB2* gene. It involves multiple systems and the clinical features include delayed growth, delayed mental development, delayed language development, craniofacial malformations (cleft palate, high palatal arch, cleft uvula and small jaw), abnormal tooth alignment and size, thinning hair, behavioral abnormalities (autistic, hyperactive and aggressive behavior), tumor progression and some rare manifestations, such as hypotonia, feeding difficulties, seizures and malformations of the bones, heart and kidneys (1-4).

The *SATB2* gene (OMIM:608148) located in the 2q33 region is ~191 kb long. It contains 12 exons, encodes a DNA-binding protein containing 733 amino acids specifically bound to the AT sequence, is highly homologous between species (5), is involved in neuronal evolution and osteoblast differentiation (6) and plays a key role in craniofacial, skeletal and brain development. Among the cases of *SATB2*-associated syndromes reported in other countries, 61% are attributed to *SATB2* heterozygous pathogenic variants, involving variants with heterozygous deletions of chromosome 2q33.1 of the *SATB2* gene (22%), variants with mutations or duplications of *SATB2* gene base loci (9%) and the remaining pathogenic variants with a reported association with chromosomal translocation and disruption of chromosome 2q33.1 breakpoints (7). Homology analysis revealed that the SATB2 protein contains two CUT structural domains: CUT1 contains amino acids 350-437, which are involved in nuclear chromatin initiation and CUT2 contains amino acids 479-557, which promote the dissociation of *SATB2* gene from specific nuclear chromatin. These two structural domains are the central nuclear matrix-binding regions of the SATB2 protein, which regulates gene expression by recognizing the sugar-phosphate structure of double-stranded DNA and binding to specific matrix-binding regions. The SATB2 protein functions through chromosomal modifications and by interacting with other proteins and ligand receptors (8).

A child with delayed mental development and delayed language development was investigated for a genetic cause. So, in the present study, medical exome sequencing was

performed and, to verify the suspected pathogenic locus, Sanger sequencing was performed for both the child and parents. The results suggested the presence of a suspected pathogenic *de novo* repetitive insertional shift mutation in the *SATB2* gene and the patient was diagnosed as having SAS in combination with the clinical phenotype.

Materials and methods

Ethics statement. The present study was approved by Ethics Committee of the First Hospital of Jilin University (approval number: 2021-485). All procedures performed in studies involving human participants were in accordance with the ethical standards of the institutional and/or national research committee and with the 1964 Helsinki declaration and its later amendments or comparable ethical standards. Written informed consent was obtained from the parents.

Subjects. The proband was an 8-year-old male child delivered at full term by normal delivery. He was brought to the First Hospital of Jilin University for delayed growth, delayed mental development and speech disorder. At the time of presentation, the child underwent a detailed medical examination with the following findings: Height, 120 cm; weight, 19.3 Kg; head circumference 43 cm; teeth, dysplasia and disorder of arrangement. Since his parents wanted to have another child, they wanted to find the genetic cause behind his presentation. A karyotype test with 320-400 bands performed previously had found no abnormalities. Furthermore, the brain parenchyma in the head MRI scan, the amino acid and acylcarnitine profiles, the urine organic acid analysis and the EEG test were all normal. Upon inquiry, the parents reported no family history of any genetic disease. For a genetic examination, 2 ml of peripheral blood sample was taken from the child as well as the parents after obtaining their written informed consent. The blood was anticoagulated with EDTA and stored at 4˚C.

Target sequence capture and sequencing. The genomic DNA from the peripheral blood of the patient and his parents was extracted using the QIAamp Blood DNA Mini kit (Qiagen GmbH). The concentration and purity of the sample DNA were detected using a UV-240 UV spectrophotometer. The fragmented DNA was then screened by magnetic beads and the screened fragments measured 280-320 bp, with the ends filled and the base 'A' added at the 3' end to make the fragments compatible with the 3' end of the fragment. After amplification and purification by ligation-mediated PCR, the library of a single subject sample was constructed. A customized gene capture probe (MGIV4 59M; MGI) was used to hybridize 10-20 labeled patient DNA libraries at 47˚C for 16-24 h. Probe washing and elution reactions were performed after hybridization, followed by post-PCR reactions of the captured samples. The libraries were tested for fragment size and concentration using Agilent 2100 Bioanalyzer (Agilent Technologies, Inc.) and a BMG microplate reader; after passing the test, libraries requiring different data amounts were used for pooling and quantification. Then, the pooling libraries were subjected to single-stranded cyclization. After making a DNA nanoball (DNB), the libraries were sequenced using a high-throughput sequencer, MGISEQ-2000 (MGI) with PE100+10 type and the raw sequencing data were obtained after sequencing.

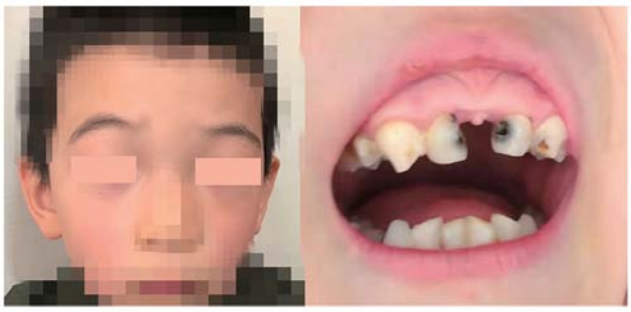

Figure 1. The proband's face and teeth.

Sequence analysis. After the data were offloaded, they were analyzed. First, the sequencing quality of raw data (raw reads) was evaluated and the low-quality and junction-contaminated reads were eliminated. Then, sequence alignment was performed with the Burrows-Wheeler Aligner (BWA) software (version 0.7.17; https://bio-bwa.sourceforge.net/) and HG19/HG20 human genome reference sequences and the sequence capture performance was simultaneously evaluated. Single nucleotide variant and InDel (insertion and deletion) search was performed with the Genome Analysis Toolkit (GATK) software (version 4.1.9.0; https://gatk.broadinstitute.org/hc/en-us) to generate base polymorphism results in the target region and subsequently databases (NCBI dbSNP (build 151; http://www.ncbi.nlm.nih.gov/SNP), 1000 human genome dataset (phase 3; https://www.internationalgenome.org/) and database of 100 Chinese healthy adults (phase I; http://cmdb.bgi.com/) were compared and the suspected mutations were annotated and screened for.

Sanger sequencing validation. The suspected pathogenic mutations identified by high-throughput sequencing were verified by Sanger sequencing of the patient and his parents and primers were designed upstream and downstream of exon 8 of the *SATB2* gene: forward primer sequence, GTCAGTGGTTTCTGTCTTGGC and reverse primer sequence, GTCAGTGGTTTCTGTCTTGGC. PCR amplification was performed. PCR reaction system was as follows: Total volume was 25 μl, including 2 X PCR MasterMix (Promega Corporation; 12.5 μl), dNTPs (3 μl), ddH2O (5.2 μl), upstream and downstream primers (1 μl each), DNA template (2 μl) and LA taqase (0.3 μl). Reaction conditions were as follows: Pre-denaturation at 95˚C for 5 min, denaturation at 95˚C for 30 sec, annealing at 68˚C for 30 sec and extension at 72˚C for 30 sec for 12 cycles. This was followed by the amplification step, wherein the sample was subjected to 94˚C for 30 sec, 58˚C for 30 sec, 72˚C for 30 sec for 35 cycles, which was followed by 72˚C extension for 5 min. Next, 1.5% agarose gel was prepared and then 2 μl of loading buffer was mixed with 4 μl of DNA amplification product. After that, Sanger sequencing was performed using the ABI3730XL (Applied Biosystems; Thermo Fisher Scientific, Inc.) sequencer and the results were compared with the hg19 reference sequence in

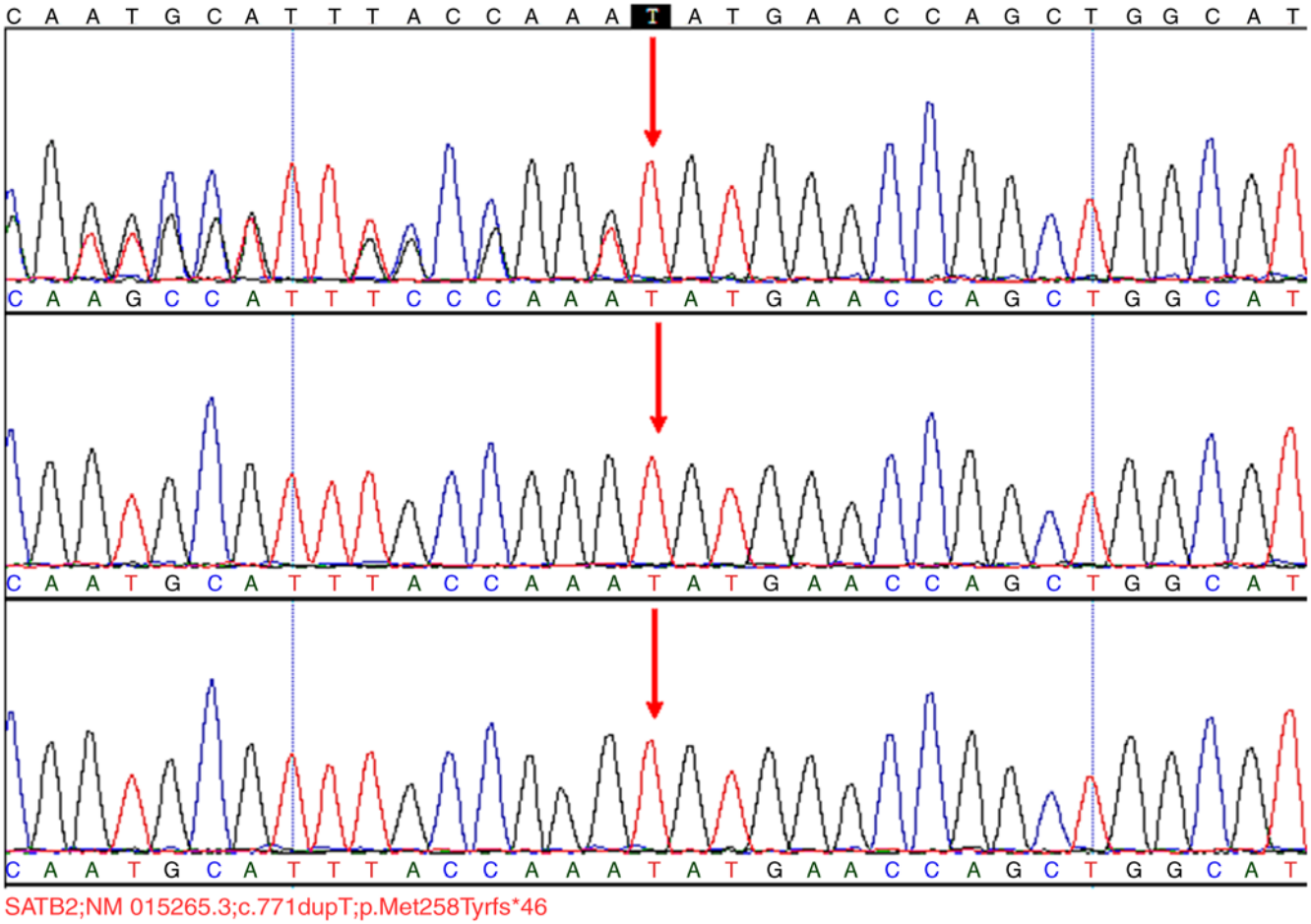

Figure 2. Sanger sequencing map of the *SATB2* gene in the child and his parents, suggesting a *de novo* heterozygous repeat insertional shift mutation in the *SATB2* gene c.771dupT (p.Met258Tyrfs*46) in the proband.

University of California Santa Cruz (UCSC) Genome Browser (https://genome.ucsc.edu/) to verify the results of gene chip capture and high-throughput sequencing.

Copy number variation (CNV) detection. The acquired sequenced segments were compared by BWA and UCSC hg19 human reference genome to remove duplicates. InDel and genotyping. ExomeDepth was used to detect CNV at the exon level.

Chromosomal karyotype analysis. After obtaining informed consent, peripheral blood samples were drawn from the parents of the patient. Then, peripheral blood lymphocytes were routinely cultured, produced and G-banded and 50 mid-phase divisions were counted microscopically and analyzed for five karyotypes.

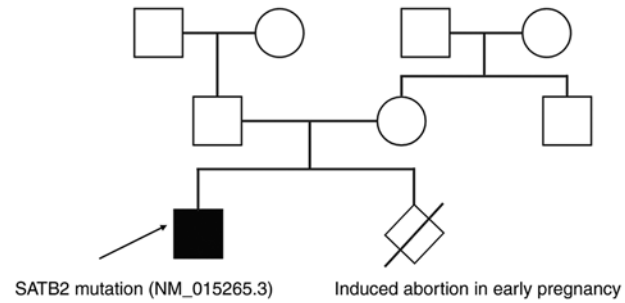

Figure 3. Family pedigree of this child with *SATB2* mutation (NM_015265.3). Squares indicate males, circles indicate females, the black symbol indicates an affected member, the diamond means the gender is not known, the diagonal line through a symbol indicates that the person is deceased, white symbols indicate unaffected members and the arrow indicates the proband.

Protein structure prediction with AlphaFold. AlphaFold is a deep neural network developed by DeepMind that predicts the 3D structure of a protein from its amino acid sequence (9). AlphaFold can predict the distance distribution between each pair of amino acids in the protein and the angle between the chemical bonds that connect them, then aggregates the measurement results of all pairs of amino acids into 2D distance histograms. The convolutional neural network can learn from these pictures and subsequently construct the 3D structure. The Fasta file format of the acquired protein sequence wase first downloaded, then submitted to the super-computer center for AlphaFold modeling. The structured model needs to be assessed by the ERRAT program (version saves6.0; https://saves.mbi.ucla.edu/), which refers to the calculation of the number of non-bond interactions between different atomic types within the range of 0.35 nm, the higher the overall quality factor value indicates a greater resolution of the crystal structure.

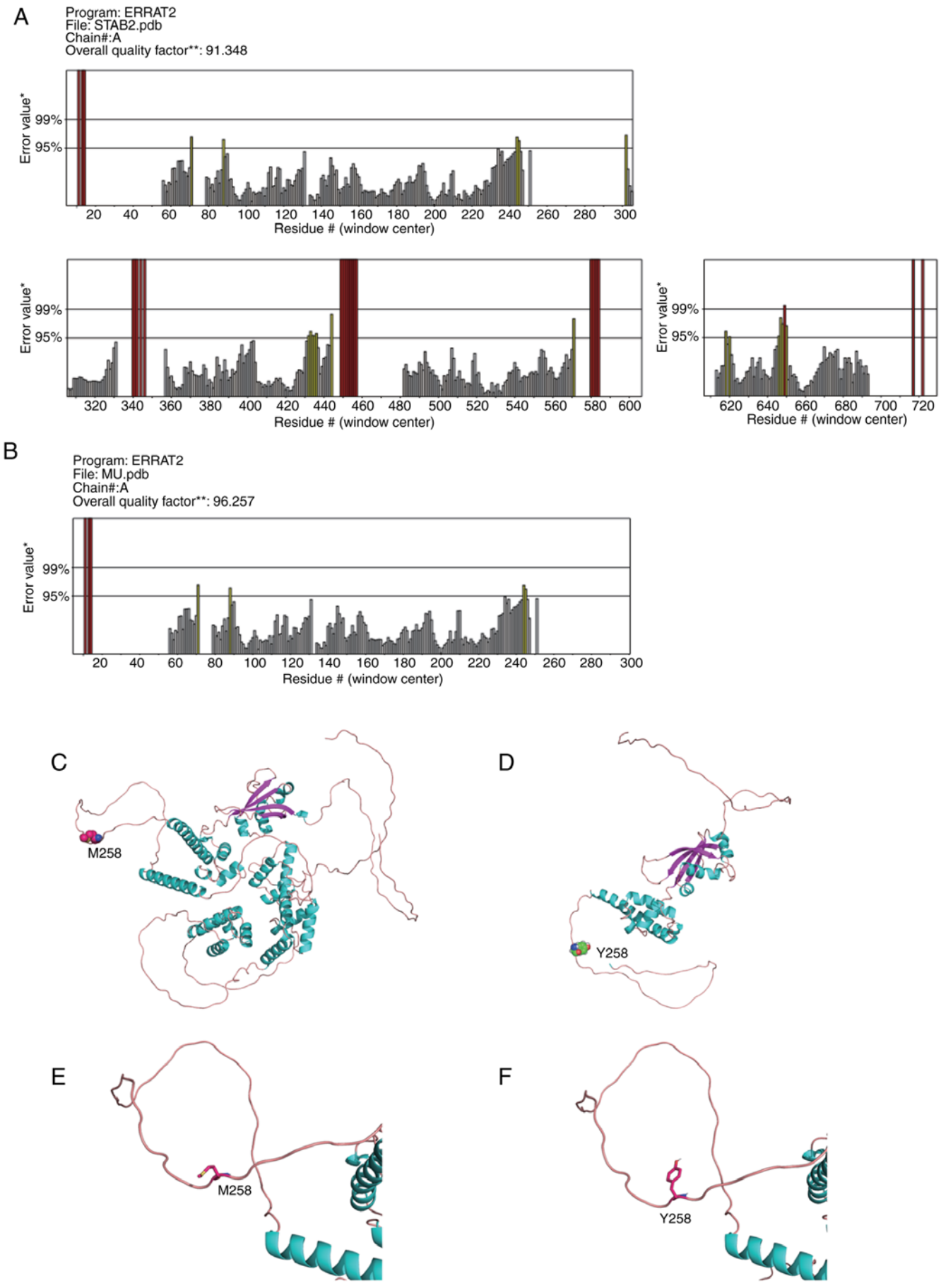

Figure 4. Protein structure prediction by AlphaFold. (A) ERRAT validation of STAB2 protein. (B) ERRAT validation of mutant protein. The three-dimensional structure of (C) the mutant protein and (D) STAB2 protein. (E and F) The property changes of amino acids in the mutant protein. STAB2, special AT-rich binding protein 2.

Table I. Phenotype of 40 cases with *SATB2* mutation including previous reports and the present study.

Author, year	Patients	Mutation	Age	Sex	Exon	Intellectual disability	Language disability	Facial deformity	Palate	Micrognathia	High palatine arches	Dental deformity	Abnormal behavior	Growth delay	Hypotonia	Epilepsy	Feeding difficulties	(Refs.)
Zarate YA *et al*, 2018	1	c.124G>T (p.G42*)	5	F	3	Y	Y(L)	Y	N	N	N	Y	N	N	Y	N	N	(18)
Zarate YA *et al*, 2021	2	c.257T>G (p.L86R)	5	M	4	Y	NR	Y	NR	NR	NR	Y	N	NR	NR	Y	NR	(20)
Zarate YA *et al*, 2021	3	c.337C>T (p.G113*)	5	F	4	Y	NR	Y	NR	NR	NR	Y	N	NR	NR	N	NR	(20)
Scott J *et al*, 2018	4	c.346G>C (p.G116R)	1	F	4	Y	Y(L)	Y	N	N	Y	Y	N	Y	Y	N	Y	(21)
Zarate YA *et al*, 2015	5	c.346+2T>G (p.Gly115 fs*15)	7	M	4	Y(mild)	Y(L)	Y	Y	Y	NR	Y	NR	NR	NR	Y	NR	(22)
Zarate YA *et al*, 2017	6	c.400delG (p.A134H fs*17)	4	F	5	Y	Y(A)	Y	N	N	N	Y	Y	N	Y	N	Y	(23)
Zarate YA *et al*, 2017	7	c.482delA (p.K161S fs*19)	10	M	6	Y	Y(L)	Y	Y	N	N	Y	Y	N	Y	N	Y	(23)
Zarate YA *et al*, 2021	8	c.546G>C (p.G116R)	5	F	6	Y	Y	Y	NR	NR	NR	Y	Y	NR	NR	N	NR	(20)
Zarate YA *et al*, 2017	9	c.583dupT (p.C195L fs*14)	5	M	6	Y	Y(A)	Y	Y	N	N	Y	Y	Y	Y	N	Y	(23)
Zarate YA *et al*, 2017	10	c.715C>T (p.R239*)	36	M	8	Y(S)	Y(L)	Y	Y	Y	NR	Y	N	NR	NR	Y	NR	(23)
Leoyklang P *et al*, 2007	11	c.715C>T (p.R239*)	3	F	8	Y(S)	Y(A)	Y	N	Y	NR	Y	Y	NR	NR	N	NR	(24)
Yamada M *et al*, 2019	12	c.715C>T (p.R239*)	7	F	8	Y	Y(A)	Y	Y	N	NR	Y	NR	NR	NR	NR	NR	(25)
Zarate YA *et al*, 2017	13	c.748C>T (p.Q250*)	32	M	8	Y(S)	Y(A)	Y	Y	N	NR	Y	NR	NR	NR	Y	NR	(23)
This study	14	c.771dupT (p.M258Y fs*46)	8	M	8	Y	Y(A)	Y	N	Y	Y	Y	Y	Y	Y	N	Y	This study

Table I. Continued.

Author, year	Patients	Mutation	Age	Sex	Exon	Intellectual disability	Language disability	Facial deformity	Palate	Micrognathia	High palatine arches	Dental deformity	Abnormal behavior	Growth delay	Hypotonia	Epilepsy	Feeding difficulties	(Refs.)
Zarate YA *et al*, 2017	15	c.816delT (p.H273T fs*21)	13	M	8	Y	Y(L)	Y	N	N	N	Y	Y	N	Y	N	Y	(23)
Kikuiri T *et al*, 2018	16	c.847C>T (p.R283*)	19	F	8	Y	Y(A)	Y	Y	N	NR	Y	Y	NR	NR	NR	NR	(26)
Zarate YA *et al*, 2021	17	c.847C>T (p.R283*)	6	M	8	Y	Y(L)	Y	N	N	Y	Y	N	N	Y	N	Y	(20)
Zarate YA *et al*, 2015	18	c.847C>T (p.R283*)	4	M	8	Y(M)	Y(A)	Y	N	N	NR	Y	NR	NR	Y	N	NR	(22)
Zarate YA *et al*, 2021	19	c.997C>T (p.G333*)	5	F		Y	NR	Y	NR	NR	NR	Y	Y	NR	NR	N	NR	(20)
Rauch A *et al*, 2012	20	c.1142T>G (p.V381G)	3	F	8	Y(S)	Y	Y	Y	N	NR	Y	NR	NR	NR	Y	NR	(27)
Zarate YA *et al*, 2021	21	c.1165C>T (p.A389C)	5	F		Y	Y	Y	NR	NR	NR	Y	Y	NR	NR	Y	NR	(20)
Lin M *et al*, 2019	22	c.1166G>A (p.R389H)	4	M	8	Y	Y	Y	Y	N	N	Y	NR	NR	NR	NR	NR	(28)
Zarate YA *et al*, 2015	23	c.1171C>T (p.Q391*)	3	M	8	Y(M)	Y(A)	Y	Y	Y	NR	Y	NR	NR	NR	N	NR	(22)
Lee JS *et al*, 2016	24	c.1186G>C (p.E396Q)	1.5	F	9	Y	Y(L)	Y	Y	Y	NR	Y	Y	NR	Y	NR	NR	(29)
Zarate YA *et al*, 2021	25	c.1195C>T (p.A399C)	7	M		Y	NR	Y	NR	NR	NR	Y	Y	NR	NR	N	NR	(20)
Zarate YA *et al*, 2017	26	c.1255C>T (p.Q419*)	5	M	9	Y	Y(L)	Y	Y	N	N	Y	Y	Y	Y	N	Y	(23)
Lv HY *et al*, 2018	27	c.1285G>A (p.R429*)	3	F	9	Y(S)	Y(A)	Y	Y	Y	NR	Y	Y	NR	NR	NR	NR	(19)
Bengani H *et al*, 2017	28	c.1285C>T (p.R429*)	4	M	9	Y	Y	Y	N	N	NR	Y	NR	NR	Y	Y	NR	(12)
Zarate YA *et al*, 2017	29	c.1286G>A (p.R429Q)	14	M	9	Y	Y(A)	Y	N	N	Y	Y	Y	N	Y	Y	N	(23)
Zarate YA *et al*, 2017	30	c.1286G>A (p.R429Q)	3	M	9	Y	Y(A)	Y	N	N	Y	Y	Y	Y	Y	N	Y	(23)
Mei DQ *et al*, 2019	31	c.1300C>T (p.Q434*)	8	F	9	Y	Y	Y	N	Y	NR	Y	NR	NR	NR	Y	NR	(30)

Table I. Continued.

Author, year	Patients	Mutation	Age	Sex	Exon	Intellectual disability	Language disability	Facial deformity	Palate	Micrognathia	High palatine arches	Dental deformity	Abnormal behavior	Growth delay	Hypotonia	Epilepsy	Feeding difficulties	(Refs.)
Zarate YA *et al*, 2021	32	c.1329_1347 dup19 (p.S450G fs*32)	4	F	9	Y	NR	Y	NR	NR	NR	Y	N	NR	NR	N	NR	(20)
Bengani H *et al*, 2017	33	c.1375C>T (p.R459*)	2	F	9	Y	Y(L)	Y	Y	Y	NR	Y	Y	NR	NR	NR	NR	(12)
Kikuiri T *et al*, 2018	34	c.1478_ 1479del (p.Q493R fs*19)	16	M	10	Y	Y(A)	Y	Y	N	NR	Y	NR	NR	NR	NR	NR	(26)
Zarate YA *et al*, 2017	35	c.1728delT (p.E577S fs*47)	6	M	11	Y	Y(A)	Y	N	N	Y	Y	Y	N	Y	N	Y	(23)
Kikuiri T *et al*, 2018	36	c.1741-1G>A	19	F	12	Y	Y(A)	Y	Y	Y	NR	Y	NR	NR	NR	N	NR	(26)
Zarate YA *et al*, 2017	37	c.1945dupT (p.S649fs*40)	5	M	12	Y(S)	Y(A)	Y	Y	Y	NR	Y	NR	NR	NR	N	NR	(23)
Zarate YA *et al*, 2017	38	c.1964C>T (p.P655L)	6	F	12	Y	Y(A)	Y	N	N	Y	Y	Y	N	Y	N	Y	(23)
Boone PM *et al*, 2016	39	c.2018dupA (p.H673fs)	15	M	12	Y(S)	N	Y	Y	Y	NR	Y	NR	N	NR	NR	NR	(31)
Yamada M *et al*, 2019	40	c.2104delG (p.D702T fs*38)	9	F	12	Y	Y(A)	Y	Y	N	NR	Y	NR	Y	NR	NR	NR	(25)

F, female; M, male; Y, yes; N, no; NR, no record; Y(S), yes and severe; Y(M), yes and moderate; Y(A), yes and absent; Y(L), yes and limited.

Results

The phenotypic progression of the child. The phenotypic progression of the child was as follows. He was born at 39-week gestation without obvious abnormality. He could sit at 6 months and walk without support at 26 months. However, at the time of writing, the child was 8 years old; his walk was not stable and he remained non-verbal. His height, weight and head circumference were 120 cm, 19.3 kg and 43 cm, respectively, with a body mass index (BMI) of 13.4. His limbs were long and thin and both knee joints were large and had cavities. He showed a significant developmental delay in terms of intelligence, particularly when compared with other children of his age. Further, he showed severe adaptability retardation, poor cognition and understanding abilities and could only understand simple commands. He showed severely impaired language development, which manifested as absent language function. Moderate lag was noted in grand motor and fine motor function. His walk was not steady with his forward-set posture and he could not run or jump. In terms of cephalic and facial abnormalities, both his eyebrows were thin and curved, bilateral downward slanting eye fissures were present and he had hypoplastic, crowded teeth, a high jaw arch, a small, pointed lower jaw with backward tilt (Fig. 1) and a flat occipital bone. He was not epileptic but showed excitable behavior, with frequent episodes of crying, hyperactivity, timidity and restlessness, as well as poor bowel awareness.

Results of genetic testing. Genetic testing of blood samples from the child and his parents revealed that the exon 8 of the *SATB2* gene had a c.771dupT (p.Met258Tyrfs*46) *de novo* repeat insertional shift mutation, which resulted in a mutation from methionine to tyrosine at the amino acid site 258 (Project number: PRJNA916183, database link: https://www.ncbi.nlm.nih.gov/bioproject/PRJNA916183). Consequently, this shift mutation altered all amino acids after site 258 and led to the production of a truncated protein with 46 amino acids missing. The parents of the child harbored no mutation at this locus (Fig. 2). The family pedigree of this child was shown in Fig. 3. The mutation identified in *SATB2* gene (NM_015265.3), which is transcript variant 2, has not been reported in the search from the OMIM database (https://omim.org/) or PubMed database (https://www.ncbi.nlm.nih.gov/pmc/), NCBI-Nucleotide (https://www.ncbi.nlm.nih.gov/nucleotide/) showed that *SATB2* NM_015265.3 mRNA transcript variant 2 contains 12 exons.

Mutation pathogenicity assessment. To the best of the authors' knowledge, the *STAB2* gene c.771dupT (p.Met258Tyrfs*46) variant detected in this case is novel. According to the American College of Medical Genetics and Genomics guidelines (10), this variant was consistent with PVS1 and PM2 in the guidelines and was suspected to be a pathogenic variant.

Protein structure prediction. The modeling scores of STAB2 and mutant protein were 91.348 and 96.257, respectively. For the STAB2 protein, the constructed protein structure has high reliability and can be used as a template for subsequent studies according to Ramachandran plot and VERFY-3D score (11) (Fig. 4A). For the mutant protein, the evaluation score was greater than 95%, which indicated high reliability and can be used as a template for subsequent studies (Fig. 4B). The three-dimensional structure of STAB2 protein consisted of 22 α-helical structures, 4 β-folds and 10 LOOP-regions. However, the mutation of p.Met258Tyrfs*46 in *STAB2* leads to the premature termination of protein translation. The mutant protein contained only 6 α-helical structures, 4 β-folds and 4 LOOP-regions, thus causing a large amount of missing structure (Fig. 4C and D). The wild-type protein sited in 258 is a nonpolar uncharged methionine, while the p.Met258Tyrfs*46 mutation results in the replacement of methionine at position 258 by tyrosine, which was large, polar and uncharged, thus increasing the aromaticity and polarity of the protein. Property changes of these amino acids may lead to alternation in the structure and function of the mutant protein (Fig. 4E and F).

Table II. Phenotype analysis of 40 cases with SATB2 single nucleotide variants.

Phenotype	Number (%)
Intellectual disability	100% (40/40)
Severe	60% (6/10)
Moderate	30% (3/10)
Mild	10% (1/10)
Language disability	97.1% (34/35)
Absent	64.3% (18/28)
Limited	35.7% (10/28)
Facial deformity	100% (40/40)
Palate	57.6% (19/33)
Micrognathia	36.4% (12/33)
High palatine arches	50% (7/14)
Dental deformity	100% (40/40)
Abnormal behavior	73.1% (19/26)
Delayed growth	40% (6/15)
Epilepsy	29% (9/31)

CNV analysis at the exon level. CNV analysis at the exon level did not detect pathogenic chromosomal CNV variants of more than 1M associated with the phenotype of the preexisting patient.

Karyotype findings. No abnormal karyotypes (320-400 bands) were found in the child and the parents' chromosome Giemsa staining bands.

Discussion

The case reported here is of a *de novo* heterozygous repeat insertional shift mutation in c.771dupT (p.Met258Tyrfs*46) which resulted in a mutation from methionine to tyrosine at the amino acid site 258 and this shift mutation affected the alteration of all amino acids after site 258 (affected protein description confirmed from database https://mutalyzer.nl/), thus resulting in a truncated protein. This truncated protein had 46 amino acids missing and structural alterations so substantial that 2/3 of amino acids were different from those of a normal

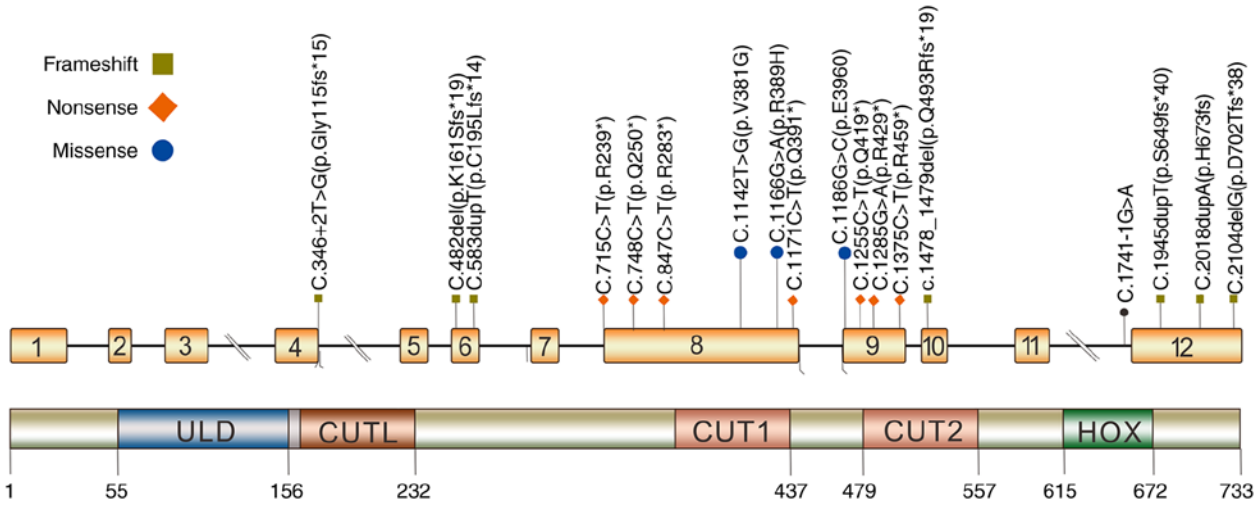

Figure 5. Distribution of *SATB2* gene variants in SAS patients with cleft palate. SAS, special AT-rich binding protein 2-associated syndrome.

protein chain. Furthermore, the two key CUT structures of the SATB2 protein were destroyed and thus the mutated protein was probably non-functional, leading to a typical clinical phenotype of the *SATB2*-associated syndrome in the child. Furthermore, the diagnosis of *SATB2*-associated syndrome was established based on considerations of both the phenotype and genotype of the child. The existing *SATB2* mutations found in ClinVar were *SATB2* NM_001172509.2 transcript variant 1 (https://www.ncbi.nlm.nih.gov/clinvar), the present study identified the *SATB2* gene mutation (NM_015265.3), which is transcript variant 2 and has not been found through PubMed database (https://www.ncbi.nlm.nih.gov/pmc/). NCBI-Nucleotide showed that *SATB2* NM_001172509.2 mRNA transcript variant 1 and *SATB2* NM_015265.3 mRNA transcript variant 2 contain 11 and 12 exons, respectively. This case analysis helps expand the spectrum of mutations in the *SATB2* gene.

The typical clinical manifestations of SAS include delayed intellectual and language development, small jaw, dental deformity and cleft palate or high jaw arch, among others. The present study retrieved 39 previously reported cases of SAS caused by *SATB2* base mutations with available data on clinical phenotypes of the patients, including the case reported here, and the phenotypes of all 40 cases are detailed in Table I. The detailed phenotypic distribution of these 40 cases is shown in Table II. Delayed intellectual development, delayed language development, facial deformity and dental deformity were the typical clinical manifestations of SAS, accounting for 100, 97.1, 100 and 100%, respectively. Bengani *et al* (12) reported that 16 out of 20 patients with *SATB2* mutation were almost or completely non-verbal. This suggests that severely impaired or absent speech is the most characteristic manifestation of the disease. Intellectual disability has a higher rate of epistasis and varying degrees of intellectual disability have been reported from the deletion/mutation of this gene. Corticocortical projection neurons occupy the superficial layers of the cerebral cortex and extend axons to the midline to form the corpus callosum. Under normal physiological conditions, the *SATB2* gene is expressed in corticocortical projection neurons (13). However, SATB2 protein deficiency prevents the normal extension of axons to the corpus callosum, thus resulting in abnormal neuronal migration and projection (14). Therefore, intellectual disability and language dysfunction are hypothesized to be associated with defective axonal projection and impaired cortical neuronal migration; furthermore, the language dysfunction noted in such patients is presumed to be neurological language dysfunction.

In addition to severe language dysfunction and moderate-to-severe mental development delay, the patient also had micromaxillary and dental malformations typical of SAS (Fig. 1). These malformations may be associated with the involvement of *SATB2* in transcriptional regulation and chromatin remodeling and its importance in bone and craniofacial development. Zhang *et al* (15) found that the expression of osteoblast-specific genes (Runx2, Atf4 and SOX9) was downregulated by mutations in the *SATB2* gene and this consequently hindered bone differentiation and repair. Gong *et al* (16) showed that loss of the *SATB2* gene caused poor bone mineralization in a mouse model, resulting in poor limb development and increased bone fragility. Britanova *et al* (17) also proposed that a loss-of-function mutation in the *SATB2* gene causes increased apoptosis of the progenitor cells responsible for jaw bone development and downregulates the genes involved in craniofacial development (Pax9, Alx4 and Msx1), thus causing maxillofacial deformities as well as dental malformations, such as abnormal, uneven tooth spacing, tooth loss and malocclusion. Therefore, dental malformations are considered characteristic of *SATB2*-associated syndromes.

In contrast to the above phenotypes, cleft palate does not show high penetrance and our patient did not show cleft palate and only had a high osprey arch. An *SATB2*-knockout mouse model showed cleft palate in ~25% cases (18) and cleft palate was found in nearly 50% of SAS patients in a previous study (19). Among the 40 patients analyzed in the present study, 19 had cleft palate and 14 did not have cleft palate. For 7 patients, this aspect was not documented (Tables I and II); outlier rates corroborated previous reports (18,19). In the 19 cases with cleft palate, the mutated loci causing cleft palate was further analyzed (Fig. 5) and found them distributed on exons 4, 6, 8, 9, 10 and 12 without any evident mutation hotspots; the mutation type varied, such as shift mutations,

nonsense mutations, missense mutations and splice mutations. In addition, it was found that mutations in the same locus (e.g., c.715C >T and c.847C>T) could manifest with or without cleft palate in patients. Therefore, the formation of a cleft palate is hypothesize to be also influenced by environmental or other factors. In addition, to the best of the authors' knowledge, the phenotype of this child (thinly curved brow and flat occipital bone) has not been reported as a consequence of a mutated *SATB2* gene in the literature thus far; therefore, it may be another rare phenotype caused by a mutation of this gene. Alternatively, the presence of this phenotype may have been overlooked in reports thus far and thus deserves further investigation and greater attention in subsequent cases.

The present study suggested that severely impaired language development, facial dysmorphism and varying degrees of delayed intellectual development are the most characteristic phenotypes of SAS. If these three manifestations are noted in early clinical stages with or without epilepsy, cleft palate, delayed growth and hyperactivity, SAS should be suspected first and the patient should be checked for pathogenic mutations or deletions in the *SATB2* gene to verify the diagnosis.

There are some limitations of the present study. First, although it identified the new SATB2 gene mutation with transcript variant 2, no relevant studies about its role and underlying mechanism were reported, Hence, the specific role and molecular mechanism of SATB2 gene mutation (transcript variant 2) related to the abnormal phenotypes of SAS warrants further study. Second, the present study did not test whether the mutant form of the protein was expressed. Finally, the treatment and prognosis of patients with SATB2-associated syndrome needs to be explored further.

Taken together, using high-throughput sequencing technology, the present study identified a case of *SATB2*-associated syndrome caused by a *de novo* heterozygous repeat insertional shift mutation in the *SATB2* gene. The findings expanded the spectrum of mutations in the *SATB2* gene. Furthermore, the observations provided detailed notes on the clinical phenotype of this child. The present study comprehensively explored the effect of this mutation on the protein structure and its relationship with the clinical phenotype. Furthermore, it retrieved data on and analyzed the phenotypic distribution of 40 cases of SAS, including the case reported in the present study, with a focus on the distribution characteristics of the cleft palate-causing mutation loci. Accordingly, the present study concluded that severely impaired language development, facial dysmorphism and varying degrees of delayed intellectual development are the most characteristic phenotypes of SAS. It is hoped these findings provide valuable information for clinicians to deepen their understanding of this disease.

Acknowledgements

Not applicable.

Funding

This study was supported by the National Natural Science Foundation of China (grant no. 82201847) and the Science and Technology Department of Jilin Province (grant nos. 20220204020YY, YDZJ202201ZYTS085 and YDZJ202201ZYTS027).

Availability of data and materials

The datasets generated and analyzed during the present study are available from the corresponding author on reasonable request.

Authors' contributions

QL and LJC performed most of the investigation, data analysis and wrote the manuscript; NNF contributed to collection and collation of the data and references. All authors have read and approved the final manuscript. QL and LJC confirm the authenticity of all the raw data.

Ethics approval and consent to participate

The present study was approved by the ethics committee of the First Hospital of Jilin University (approval number: 2021-485). All procedures performed in studies involving human participants were in accordance with the ethical standards of the institutional and/or national research committee and with the 1964 Helsinki declaration and its later amendments or comparable ethical standards.

Patient consent for publication

Written informed consent was obtained from the parents of the proband.

Competing interests

The authors declare that they have no competing interests.

References

1. Döcker D, Schubach M, Menzel M, Munz M, Spaich C, Biskup S and Bartholdi D: Further delineation of the SATB2 phenotype. Eur J Hum Genet 22: 1034-1039, 2014.
2. Mouillé M, Rio M, Breton S, Piketty ML, Afenjar A, Amiel J, Capri Y, Goldenberg A, Francannet C, Michot C, *et al*: SATB2-associated syndrome: Characterization of skeletal features and of bone fragility in a prospective cohort of 19 patients. Orphanet J Rare Dis 17: 100, 2022.
3. Inoue H, Matsushima J, Kobayashi S, Sairenchi T, Hirata H, Chida M, Ota S, Ban S and Matsumura Y: Expression of SATB2 in neuroendocrine carcinomas of the lung: Frequent immunopositivity of large cell neuroendocrine carcinoma with a diagnostic pitfall. Int J Surg Pathol 30: 151-159, 2022.
4. Shahrabi-Farahani S, Pencarinha DM and Anderson M: SATB2 immunoexpression in peripheral ossifying fibroma and peripheral odontogenic fibroma. Head Neck Pathol 16: 339-343, 2022.
5. Rosenfeld JA, Ballif BC, Lucas A, Spence EJ, Powell C, Aylsworth AS, Torchia BA and Shaffer LG: Small deletions of SATB2 cause some of the clinical features of the 2q33.1 microdeletion syndrome. PLoS One 4: e6568, 2009.
6. Dobreva G, Chahrour M, Dautzenberg M, Chirivella L, Kanzler B, Fariñas I, Karsenty G and Grosschedl R: SATB2 is a multifunctional determinant of craniofacial patterning and osteoblast differentiation. Cell 125: 971-986, 2006.
7. Zarate YA and Fish JL: SATB2-associated syndrome: Mechanisms, phenotype, and practical recommendations. Am J Med Genet A 173: 327-337, 2017.

8. Dobreva G, Dambacher J and Grosschedl R: SUMO modification of a novel MAR-binding protein, SATB2, modulates immunoglobulin mu gene expression. Genes Dev 17: 3048-3061, 2003.
9. AlQuraishi M: AlphaFold at CASP13. Bioinformatics 35: 4862-4865, 2019.
10. Richards S, Aziz N, Bale S, Bick D, Das S, Gastier-Foster J, Grody WW, Hegde M, Lyon E, Spector E, *et al*: Standards and guidelines for the interpretation of sequence variants: A joint consensus recommendation of the American college of medical genetics and genomics and the association for molecular pathology. Genet Med 17: 405-424, 2015.
11. Sneha, Pandey JP and Pandey DM: Evaluating the role of trypsin in silk degumming: An in silico approach. J Biotechnol 359: 35-47, 2022.
12. Bengani H, Handley M, Alvi M, Ibitoye R, Lees M, Lynch SA, Lam W, Fannemel M, Nordgren A, Malmgren H, *et al*: Clinical and molecular consequences of disease-associated de novo mutations in SATB2. Genet Med 19: 900-908, 2017.
13. Alcamo EA, Chirivella L, Dautzenberg M, Dobreva G, Fariñas I, Grosschedl R and McConnell SK: Satb2 regulates callosal projection neuron identity in the developing cerebral cortex. Neuron 57: 364-377, 2008.
14. Leone DP, Heavner WE, Ferenczi EA, Dobreva G, Huguenard JR, Grosschedl R and McConnell SK: Satb2 regulates the differentiation of both callosal and subcerebral projection neurons in the developing cerebral cortex. Cereb Cortex 25: 3406-3419, 2015.
15. Zhang J, Tu Q, Grosschedl R, Kim MS, Griffin T, Drissi H, Yang P and Chen J: Roles of SATB2 in osteogenic differentiation and bone regeneration. Tissue Eng Part A 17: 1767-1776, 2011.
16. Gong Y, Qian Y, Yang F, Wang H and Yu Y: Lentiviral-mediated expression of SATB2 promotes osteogenic differentiation of bone marrow stromal cells in vitro and in vivo. Eur J Oral Sci 122: 190-197, 2014.
17. Britanova O, Depew MJ, Schwark M, Thomas BL, Miletich I, Sharpe P and Tarabykin V: Satb2 haploinsufficiency phenocopies 2q32-q33 deletions, whereas loss suggests a fundamental role in the coordination of jaw development. Am J Hum Genet 79: 668-678, 2006.
18. Zarate YA, Smith-Hicks CL, Greene C, Abbott MA, Siu VM, Calhoun ARUL, Pandya A, Li C, Sellars EA, Kaylor J, *et al*: Natural history and genotype-phenotype correlations in 72 individuals with SATB2-associated syndrome. Am J Med Genet A 176: 925-935, 2018.
19. Lv HY, Zheng RJ, Wang QL, Ren PS, Jin LH, Gu XL and Li LX: SATB2-associated syndrome: A case report of a de novo nonsense mutation in satb2 from china and review of literature. Clin Lab 64: 627-637, 2018.
20. Zarate YA, Örsell JL, Bosanko K, Srikanth S, Cascio L, Pauly R and Boccuto L: Individuals with SATB2-associated syndrome with and without autism have a recognizable metabolic profile and distinctive cellular energy metabolism alterations. Metab Brain Dis 36: 1049-1056, 2021.
21. Scott J, Adams C, Simmons K, Feather A, Jones J, Hartzell L, Wesley L, Johnson A, Fish J, Bosanko K, *et al*: Dental radiographic findings in 18 individuals with SATB2-associated syndrome. Clin Oral Investig 22: 2947-2951, 2018.
22. Zarate YA, Perry H, Ben-Omran T, Sellars EA, Stein Q, Almureikhi M, Simmons K, Klein O, Fish J, Feingold M, *et al*: Further supporting evidence for the SATB2-associated syndrome found through whole exome sequencing. Am J Med Genet A 167A: 1026-1032, 2015.
23. Zarate YA, Kalsner L, Basinger A, Jones JR, Li C, Szybowska M, Xu ZL, Vergano S, Caffrey AR, Gonzalez CV, *et al*: Genotype and phenotype in 12 additional individuals with SATB2-associated syndrome. Clin Genet 92: 423-429, 2017.
24. Leoyklang P, Suphapeetiporn K, Siriwan P, Desudchit T, Chaowanapanja P, Gahl WA and Shotelersuk V: Heterozygous nonsense mutation SATB2 associated with cleft palate, osteoporosis, and cognitive defects. Hum Mutat 28: 732-738, 2007.
25. Yamada M, Uehara T, Suzuki H, Takenouchi T, Yoshihashi H, Suzumura H, Mizuno S and Kosaki K: SATB2-associated syndrome in patients from Japan: Linguistic profiles. Am J Med Genet A 179: 896-899, 2019.
26. Kikuiri T, Mishima H, Imura H, Suzuki S, Matsuzawa Y, Nakamura T, Fukumoto S, Yoshimura Y, Watanabe S, Kinoshita A, *et al*: Patients with SATB2-associated syndrome exhibiting multiple odontomas. Am J Med Genet A 176: 2614-2622, 2018.
27. Rauch A, Wieczorek D, Graf E, Wieland T, Endele S, Schwarzmayr T, Albrecht B, Bartholdi D, Beygo J, Di Donato N, *et al*: Range of genetic mutations associated with severe non-syndromic sporadic intellectual disability: An exome sequencing study. Lancet 380: 1674-1682, 2012.
28. Lin M, Yao R, Lu J, Chen W, Xu Y, Li G, Yu T, Qing Y, Jin X and Wang J: Analysis of SATB2 gene mutation in a child with glass syndrome. Zhonghua Yi Xue Yi Chuan Xue Za Zhi 36: 712-715, 2019 (In Chinese).
29. Lee JS, Yoo Y, Lim BC, Kim KJ, Choi M and Chae JH: SATB2-associated syndrome presenting with Rett-like phenotypes. Clin Genet 89: 728-732, 2016.
30. Mei DQ, Mei SY and Chen GH: A case report of SATB2-associated syndrome and review of the literature. Chin J Neurol 52: 1059-1063, 2019.
31. Boone PM, Chan YM, Hunter JV, Pottkotter LE, Davino NA, Yang Y, Beuten J and Bacino CA: Increased bone turnover, osteoporosis, progressive tibial bowing, fractures, and scoliosis in a patient with a final-exon SATB2 frameshift mutation. Am J Med Genet A 170: 3028-3032, 2016.